Lasers in Manufacturing Conference 2025

Enabling Additive Manufacturing Applications for Structural Engineering with DED-LB of High-Strength Steels

Akshay Ashok Benni[a], Pietro Antonio Martelli[b], Vasile Luchin[c], Ilchat Sabirov[b], Andrea Crosato[a], Alper Kanyilmaz[d], Ali Gokhan Demir[d], Barbara Previtali[d]

[a] *BLM S.P.A., Via Selvaregina, 30, 22063 Cantù (CO), Italy*
[b] *IMDEA Materials Institute, Getafe, 28906, Madrid, Spain*
[c] *Mimete S.r.l., Via Padania 10, 20853 Biassono (MB), Italy*
[d] *Politecnico di Milano, Via La Masa 1, 20156 Milano (MI), Italy*

Abstract

Additive manufacturing (AM) of steel is gaining traction in the construction industry, offering the ability to fabricate complex geometries and optimize resource use. Among the AM techniques, Laser-Based Powder Directed Energy Deposition (DED-LB) is notable as it provides a compromise of relatively high productivity with respect to powder bed fusion and fine resolution with respect to arc based DED processes. However, the common steel grades often encounter challenges in meeting construction requirements, including limited compatibility with conventional structural steels concerning bolted and welded assemblies. This study tackles these challenges by developing the DED-LB process with a novel high-strength steel powder feedstock. Through an extensive experimental campaign, the research evaluates the processability of the material, focusing on achieving dense and crack-free steel components. The results highlight optimized deposition strategies providing high mechanical strength, opening new possibilities for its adoption in the construction sector for medium to large sized products.

Keywords: Laser Metal Deposition, DED-LB, high strength steel, steel structures

1. Introduction

The construction sector has witnessed increased adoption of Additive Manufacturing (AM) technologies, driven by the potential of these technologies to facilitate the creation of lightweight yet complex steel structures, AM allows for the fabrication of complex geometries and components, often difficult or impossible to achieve using conventional techniques [Vafadar et al., 2023], [Chierici et al., 2024]. These methods facilitate the development of efficient and creative designs, while simultaneously reducing steel consumption. Among the various AM technologies, laser based powder directed energy deposition (DED-LB) has emerged as a promising solution for structural engineering applications, offering a balance between production efficiency and geometric precision [Svetlizky et al., 2022].

Current DED-LB research demonstrates the successful processing of various steel alloys, with a primary focus on stainless steels, tool steels, and maraging steel alloys [Gibson et al., 2021]. However, a critical research gap exists in construction applications where material compatibility is paramount. Construction steels are typically low-alloyed grades with mechanical properties between 235 MPa and 420 MPa of yield strength (designated as S235 and S420 based on their nominal yield strength), with the S355 being the most common construction steel grade. Although there is not a standardized international definition, steels with yield strength ≥460 MPa are commonly referred to as high strength steels [Tong et al., 2021]. The high strength steels commonly used in construction are the S690, S770, S890, and S960 steel grades.

Integrating AM-produced components with conventional steel structures through bolted or welded joints, requires compatible chemical compositions and mechanical properties to the traditional construction steel grades. Moreover, the construction industry's regulatory requirements and safety-critical applications demand dense, crack-free components with

good mechanical performance. Current literature lacks comprehensive studies on HSLA steel powder feedstock optimized for DED-LB.

This study addresses these research gaps by developing optimized DED-LB processes for novel high-strength steel powder feedstock specifically tailored for structural engineering applications, focusing on achieving defect-free processability and evaluating mechanical performance for construction applications.

2. Materials and methods

A novel gas atomized low alloyed steel powder feedstock (MARS700, Mimete, Biassono, Italy) with the nominal composition as described in Table 1, and powder size d_{10}=56 µm, and d_{90}=109 µm was utilized in the current work, with an AISI304L substrate measuring 10 mm in thickness.

Table 1. Nominal composition of the powder feedstock utilized in the current work

Element	C	Si	Cr	Mn	Ni	Mo	P	Fe
Nominal wt%	0.08	0.6	0.3	1.7	1.6	0.5	0.01	Bal

The deposition cell employed in the current work is a prototypical DED-LB cell (Additube, BLM Group, Cantù, Italy) at Politecnico di Milano, as shown in Figure 1. The system consists of a 6-axis anthropomorphic robot (IRB 4600 45/2.05, ABB Ltd., Zürich, Switzerland) coupled with a 2-axis positioner (IRBP A-250, ABB Ltd, Västerås, Sweden). The laser deposition head (MWO-I-Powder, KUKA AG, Augsburg, Germany) is equipped with collimation lens and focusing lens unit, with focal lengths of 129 mm and 200 mm, respectively. The powder and gas delivery system consists of a powder feeding and gas management unit (TWIN PF 2/2-MF unit, GTV Verschleißschutz GmbH, Luckenbach, Germany) coupled with a three-jet nozzle (3-JET-SO16-S, Fraunhofer ILT, Aachen, Germany). Additionally, the laser system is equipped with a multimode fiber laser source (YLS-3000, IPG Photonics, Oxford, United States) with a maximum power of 3 kW operating at 1070 nm wavelength. The feeding and process fibres feature core diameters of 100 µm and 400 µm, respectively coupled by a fibre-to-fibre coupler.

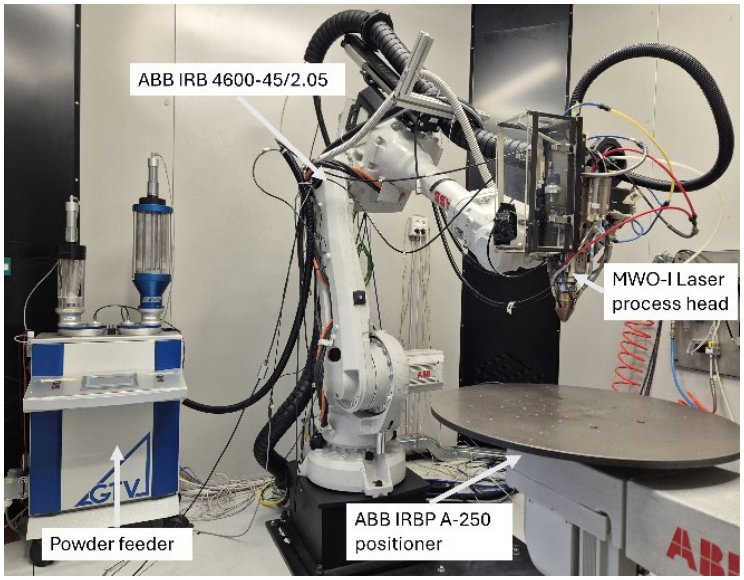

Fig. 1. The DED-LB system employed in the present study

3. Experimental campaign

The experimental campaign was structured into three phases. The initial phase was a preliminary campaign that established a process window and identified the optimal process conditions for bulk deposition. Following this, a densification study was conducted to investigate the processability of defect-free depositions with the alloy. The final stage of the experiment entailed the mechanical characterization of the specimen produced.

3.1. Process window identification

Considering the novel nature of the feedstock material, a comprehensive experimental campaign involving a single-track approach was initiated to investigate the processability of the alloy. A non-replicate full factorial experiment was conducted, with four factors at multiple levels each. The variables under investigation were the laser spot diameter (ds), laser power (P), powder feed rate (PFR), and travel speed (v). The stand-off distance (SOD), carrier, and shielding gas flow rates were held constant during the experiment. A total of 336 individual tracks, each measuring 45 mm in length, were deposited with a fixed and variable parameter set, as outlined in Table 2. A qualitative analysis was conducted to exclude tracks that were deemed to be of insufficient quality visually. The indicators for unstable depositions were inconsistent deposition with visible waviness, discoloration, and lack of deposition.

Table 2. Process parameters employed for the preliminary campaign of single tracks

Variable parameters	**Levels**
Laser spot diameter, ds [mm]	1.2; 1.6; 2
Laser power, P [W]	400; 700; 1000; 1300; 1600; 1900; 2200
Travel speed, v [mm/s]	8; 16; 24; 32
Powder feed rate, PFR [g/min]	3.3; 6.6; 9.7; 12.9
Fixed parameters	**Value**
Stand-off distance, SOD [mm]	12
Carrier flow rate, [l/min]	7.5
Shielding flow rate, [l/min]	25

Given the considerable number of single-clad depositions, an approach based on the concept of transferability was utilized, whereby the process performance of single passes can be extended to multi-pass, multi-layer depositions [Maffia et al. 2023]. Subsequently, the acceptable tracks were acquired via optical focus varying microscope, utilizing the three dimensional data obtained, a comprehensive reconstruction of a section of each track was conducted to measure the average track width (w), track height (h), aspect ratio which is the ratio of the track width to its height (AR), average contact angle (α_{avg}), productivity (Pr), and powder catchment efficiency (η_p). To avoid the formation of porosities due to lack of fusion between adjacent tracks, only the process parameters resulting in a contact angle less than 65° and an aspect ratio greater than 3 were considered. The process parameter with the best productivity (calculated as per equation 1) and powder catchment efficiency (calculated according to equation 2) was selected for the densification analysis.

$$P_r = \frac{V \cdot \rho}{t} \tag{1}$$

$$\eta_p = \frac{P_r}{PFR \cdot 60} \cdot 100 \tag{2}$$

Where, V: track volume [cm^3], t: deposition time [s], and ρ: material density [g/cm^3]

3.2. Densification analysis

Two distinct process parameter sets, designated as parameter sets 1 and 2, are employed as fixed parameter sets, derived from the outcomes of preceding sections. For parameter set 1, a laser spot of 1.2 mm, laser power of 1600 W, travel speed of 8 mm/s, and the PFR of 6.6 g/min were utilized. Similarly, for parameter set 2, a laser spot of 2 mm, laser power of 2200 W, travel speed of 16 mm/s, the PFR of 9.7 g/min, and SOD of 12 mm were utilized. While the varied parameters for both sets were: overlapping at 40% and 50% of the respective single-track widths, and z-step at 80% and 90% of the respective single-layer height. Three replicates of each unique condition were carried out, resulting in a total of 24 cubes being deposited. The meander deposition strategy was employed, utilizing an alternating layer orientation of 90°. Bulk density measurements were carried in according to ASTM B311 for the cubes deposited. While the metallographic cross section of the specimen with the highest density was analyzed for porosities.

Fig. 2. Prismatic cubes (15x15x15 mm^3) fabricated for the densification analysis

3.3. Microstructure and mechanical characterization

Based on the specimen resulting in the highest densification, samples with the optimal process parameter of laser spot diameter of 2 mm, laser power of 2.2 kW, travel speed of 16 mm/s, and the powder flow rate of 9.7 g/min were produced for microstructural and mechanical characterization. For microstructural characterization, the samples were etched with Vilella's reagent, while Vickers microhardness was conducted at an indentation force of 500 gf for a dwell time of 15 s. Tensile test was carried out in accordance with ASTM E8, in three orientations (0°,45°,90°).

4. Results

4.1. Single track campaign

Figure 3 shows the results of the single track campaign; the preliminary qualitative process window was established. As seen, the process window reveals that lower travel speed consistently provides a broader processing window across all laser spot sizes, offering more robust parameter combinations. At reduced spot sizes (1.2 mm), higher travel speeds result in inadequate depositions due to insufficient energy density to fully melt the powder feedstock being fed. In contrast, a larger laser spot size (2 mm) exhibited enhanced tolerance to higher travel speeds, demonstrating a broader process window. While higher laser powers generally enhance process stability at higher travel speed.

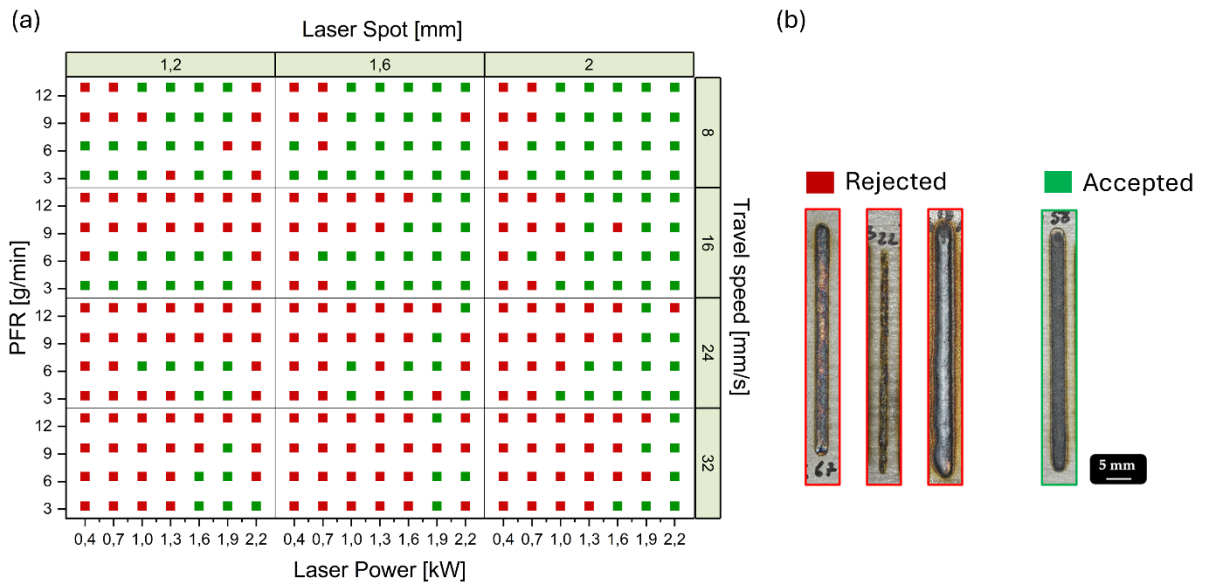

Fig. 3. (a) Result of the single track process window analysis, and (b) the qualitative criteria utilized for the selection of tracks

The results also showed an increase in both productivity and powder efficiency with increasing laser spot, laser power, and powder flow rate; however, higher powder flow rate resulted in an increase of the average contact angle. By constraining the average contact angle to a maximum threshold of 65° to prevent lack-of-fusion defects in bulk deposition processes, significant process performance can still be achieved, with deposition rates reaching up to 400 g/h and material utilization efficiencies of up to 70%.

4.2. Densification analysis

The bulk density results are summarized in Table 3. It was observed that the parameter set with a laser spot of 2 mm exhibited slightly higher densities compared to those with a 1.2 mm spot. However, all the depositions showed good densification. The metallographic cross section (see Figure 4) of the optimal condition revealed an absence of fusion defects and limited circular gas pores with relative porosity of 0.1%, demonstrating defect-free dense deposition. These results suggest that producing high-strength steel via DED-LB/P is feasible.

Table 3. Densification results for the bulk deposition

Laser spot diameter [mm]	Laser power [W]	Travel speed [mm/s]	Powder flowrate [g/min]	Overlap [%]	Zstep [%]	ρ [g/cm3]
1.2	1600	8	6.6	40	80	7.75±0.01
1.2	1600	8	6.6	40	90	7.76±0.02
1.2	1600	8	6.6	50	80	7.73±0.03
1.2	1600	8	6.6	50	90	7.76±0.02
2	2200	16	9.7	40	80	7.78±0.01
2	2200	16	9.7	40	90	7.79±0.01
2	2200	16	9.7	50	80	7.78±0.02
2	2200	16	9.7	50	90	7.78±0.01

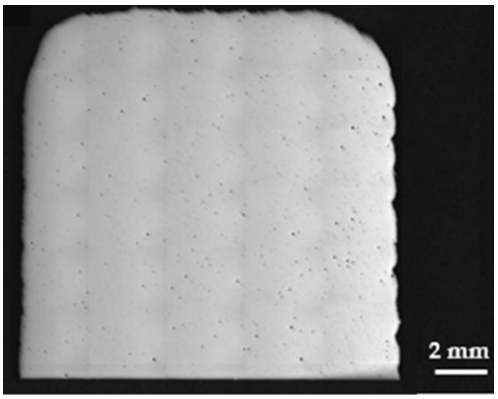

Fig. 4. Optical acquisition of the metallographic cross section under optimal conditions

4.3. Microstructure and mechanical characterization

Microstructural analysis showed larger elongated Prior Austenite Grains (PAGs) near the surface, while a finer equiaxed structure can be found in the bulk, as seen in Figure 5. The microhardness measurements obtained revealed a Vickers hardness of 277±9 $HV_{0.5}$.

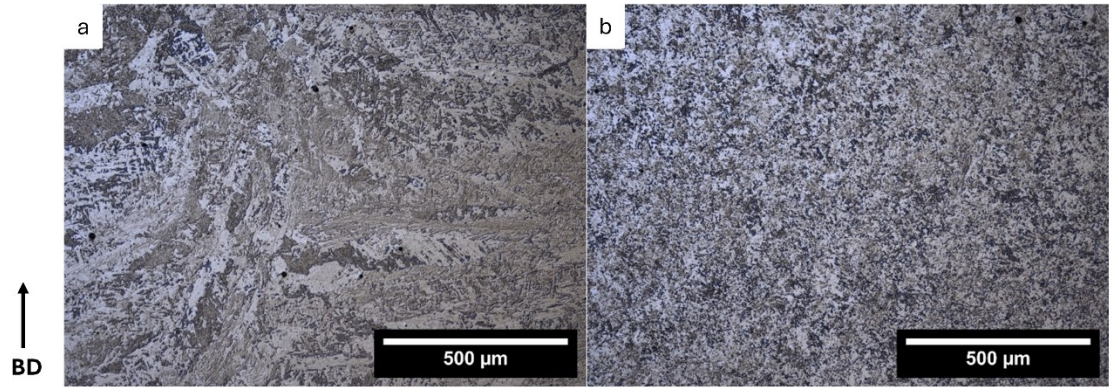

Fig. 5. Optical images of the DED-LB/p sample taken (a) near the surface and (b) in the bulk

The tensile strength measurements are summarized in Table 4. The tensile strength analysis revealed anisotropic behavior in the deposited material with a strength reduction of approximately 8% when comparing 0° to 90° orientations. Specimens oriented at 0° demonstrated the highest ultimate tensile strength (794.0±5.1 MPa), followed by 45° orientation (753.8±1.0 MPa), while 90° specimens exhibited the lowest values (731.8±17.5 MPa). Similarly, for the yield strength, the 0° specimens demonstrated the highest values (549.5±8.2 MPa), while the 90° specimens exhibited the lowest values (496.8 ± 9.5 MPa). These findings demonstrate that the deposited material achieves mechanical properties superior to those of conventional construction steels and comparable to the performance levels of high-strength steels.

Table 4. Tensile properties of deposition for three orientations

Orientation (°)	**E (GPa)**	**UTS (MPa)**	**YS (MPa)**	**$\varepsilon_{fracture}$ (%)**
0°	186.8±11.9	794.0±5.1	549.5±8.2	13.0±2.2
45°	207.3±1.0	753.8±1.0	535.5±7.6	13.6±0.9
90°	195.3±6.8	731.8±17.5	496.8±9.5	13.6±0.3

5. Conclusions

The current work focused on investigating the processability of a novel high-strength steel powder feedstock that is better compatible with the conventional construction steel for the DED-LB/p process. The work involved an extensive single-track campaign to identify a broad process window of the novel feedstock. From which process parameters were selected for bulk deposition with the view of achieving high productivity and powder efficiency. Through an extensive experimental campaign, the research evaluates the processability of the material, focusing on achieving dense and crack-free components. This research offers new possibilities for DED-LB adoption in the construction sector for medium to large-sized structural products, potentially transforming manufacturing and integrating complex structural elements within existing construction systems. The following conclusions can be made:

- The process development strategy employed, from single track qualitative feasibility to multilayer components, proved successful in producing fully consolidated components with optimal process stability.
- The high densification seen in the current work confirms the feasibility of processing high strength steel with DED-LB/p.
- The microstructure showed tempered bainitic microstructure, with large elongated prior austenite grain seen at the edges of the surface, while finer equiaxed grain structure was seen in the bulk.
- The tensile results showed anisotropy, with the 0° configuration having the higher values in terms of YS and UTS, of 549.5±8.2 MPa, and 794.0±5.1 MPa, respectively. While 496.8±9.5 MPa, and 731.8±17.5 MPa, respectively, for 90° oriented specimens.

Acknowledgements

This work has been realized as part the research project CONSTRUCTADD EU-RFCS 101057957 (http://www.constructadd.eu), funded by the European Union. Views and opinions expressed are, however, those of the authors only and do not necessarily reflect those of the European Union 920 or Research Fund for Coal and Steel. Neither the European Union nor the Research Fund for Coal and Steel can be held responsible for them.

References

Vafadar, A.; Guzzomi, F.; Rassau, A.; Hayward, K. Advances in Metal Additive Manufacturing: A Review of Common Processes, Industrial Applications, and Current Challenges. Appl. Sci. 2021, 11, 1213.https://doi.org/10.3390/app11031213

Chierici M, Demir AG, Kanyilmaz A, Berto F, Castiglioni CA, Previtali B. Hybrid manufacturing of steel construction parts via arc welding of LPBF-produced and hotrolled stainless steels. Progress in Additive Manufacturing 2024;9:471–92.https://doi.org/10.1007/s40964-023-00466-z.

I. Gibson, D. Rosen, B. Stucker, and M. Khorasani, "Additive Manufacturing Technologies," Tech. Rep., 2021. DOI: https://doi.org/10.1007/978-3-030-56127-7.

David Svetlizky, Baolong Zheng, Alexandra Vyatskikh, Mitun Das, Susmita Bose, Amit Bandyopadhyay, Julie M. Schoenung, Enrique J. Lavernia, Noam Eliaz, Laser-based directed energy deposition (DED-LB) of advanced materials, Materials Science and Engineering: A, Volume 840, 2022, 142967, ISSN 0921-5093, https://doi.org/10.1016/j.msea.2022.142967.

S. Maffia, F. Chiappini, G. Maggiani, V. Furlan, M. Guerrini, and B. Previtali, "Enhancing productivity and efficiency in conventional laser metal deposition process for Inconel 718 - part I: the effects of the process parameters," International Journal of Advanced Manufacturing Technology, Oct. 2023, doi: 10.1007/s00170-023-12196-1.

Tong L, Niu L, Ren Z, Zhao XL. Experimental research on fatigue performance of highstrength structural steel series. J Constr Steel Res 2021;183:106743. https://doi.org/10.1016/j.jcsr.2021.106743.